

Electron Ionization Mass Spectrum of Tellurium Hexafluoride

Richard A. Clark,^{*,†} Bruce K. McNamara,[‡] Charles J. Barinaga,[†] James M. Peterson,[‡] Niranjana Govind,[§] Amity Andersen,[§] David G. Abrecht,[†] Jon M. Schwantes,[†] and Nathan E. Ballou[†]

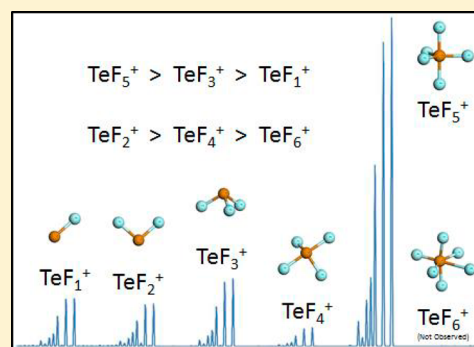
[†]National Security Directorate, Pacific Northwest National Laboratory, 902 Battelle Boulevard, Richland, Washington 99352, United States

[‡]Energy and Environment Directorate, Pacific Northwest National Laboratory, 902 Battelle Boulevard, Richland, Washington 99352, United States

[§]Environmental Molecular Sciences Laboratory, Pacific Northwest National Laboratory, 902 Battelle Boulevard, Richland, Washington 99352, United States

S Supporting Information

ABSTRACT: The electron ionization mass spectrum of tellurium hexafluoride (TeF_6) is reported for the first time. The starting material was produced by direct fluorination of Te metal or TeO_2 with nitrogen trifluoride. Formation of TeF_6 was confirmed through cryogenic capture of the tellurium fluorination product and analysis through Raman spectroscopy. The eight natural abundance isotopes were observed for each of the set of fragment ions: TeF_5^+ , TeF_4^+ , TeF_3^+ , TeF_2^+ , TeF_1^+ , and Te^+ , Te_2^+ . A trend in increasing abundance was observed for the odd fluoride bearing ions, $\text{TeF}_1^+ < \text{TeF}_3^+ < \text{TeF}_5^+$, and a decreasing abundance was observed for the even fragment series, $\text{Te}(\text{F}_0)^+ > \text{TeF}_2^+ > \text{TeF}_4^+ > \text{TeF}_6^+$, with the molecular ion TeF_6^+ not observed at all. Density functional theory based electronic structure calculations were used to calculate optimized ground state geometries of these gas phase species, and their relative stabilities explain the trends in the data and the lack of observed signal for TeF_6^+ .



1. INTRODUCTION

Fluorination of metals has been used historically as a technique for isotopic enrichment by gaseous diffusion^{1–3} and gaseous centrifugation.^{2–5} It has also been discussed as a means for chemical separation and purification,^{6–8} and more recently for nuclear forensic endeavors.^{9–11} Here, the generation of volatile metal fluorides is accomplished using nitrogen trifluoride (NF_3). NF_3 is unreactive and less hazardous than other fluorinating agents [e.g., fluorine (F_2), bromine trifluoride (BrF_3), krypton difluoride (KrF_2), and hydrofluoric acid (HF)] under ambient conditions, and these qualities make it useful for screening fluorination behavior safely.^{12–15} However, NF_3 , like all fluorinating agents, is an oxidizer and should be handled with care. Additionally, the low reactivity of NF_3 allows for selective fluorination of different species, which volatilize at specified temperatures.¹⁵ With the use of these species dependent traits, elements of a sample can be sequentially removed from a matrix, or the matrix itself volatilized, and in-line separated. Little is published concerning the reactive chemistry of NF_3 . Mass spectrometry provides one method to investigate potential metal– NF_3 adduct formation, changes in fluorination product, or product distribution relative to other fluorinating reagents.

A quadrupole mass spectrometer (QMS) with an electron ionization source (EI, formerly electron impact ionization) was directly coupled to the gas outlet of a thermogravimetric

analyzer (TGA) for analysis. The tandem setup is the first in the evolution of methodologies that would rapidly quantify isotopic variation in high performance materials that are typically encapsulated in natural and man-made matrices.

In this study, volatile tellurium hexafluoride (TeF_6) was produced from the fluorination of two forms of tellurium, tellurium metal and tellurium dioxide (TeO_2). Here, we present the first known electron ionization mass spectrum of gaseous tellurium hexafluoride.

The element tellurium (Te) has eight naturally occurring isotopes with mass numbers ranging from 120 to 130. Tellurium metal has a melting point of 450 °C and a boiling point of 988 °C, and the dioxide of tellurium melts at 733 °C and boils at 1245 °C.¹⁶ Fluorine gas reacts with the metal and dioxide to form three primary products with a product ratio depending on the reaction temperature.¹⁷ At reaction temperatures above 150 °C, the product is exclusively tellurium hexafluoride^{17,18} with melting point –37.6 °C and sublimation point –38.9 °C. At a reaction temperature of 60 °C and in the presence of oxygen, bis(pentafluorotelluryl) oxide ($\text{F}_5\text{TeOTeF}_5$)^{17–20} is reportedly formed in addition to the hexafluoride, with the $\text{F}_5\text{TeOTeF}_5$ species having a melting point at –36.6 °C and boiling point at 59.8 °C.²⁰ At

Received: February 11, 2015

approximately 0 °C reaction temperature, tellurium tetrafluoride (TeF_4) is exclusively formed.¹⁷ The tetrafluoride is a white crystalline solid at room temperature with a melting point of 129 °C. At 195 °C, TeF_4 disproportionates to form elemental Te and TeF_6 .²¹ When tellurium metal is finely powdered, fluorine reacts to form the hexafluoride even at liquid nitrogen temperatures.²² Scheele et al. showed that NF_3 begins to slowly fluorinate tellurium dioxide (TeO_2) around 260 °C with increased fluorination at 360 °C.¹³ Though other methods have been employed,^{23,24} no mass spectra of TeF_6 , TeF_4 , or $\text{F}_5\text{TeOTeF}_5$ have been reported in the literature using electron ionization mass spectrometry.

2. METHODS

Tellurium metal and tellurium dioxide were both used as starting materials in this study and were available from house chemical stocks at Pacific Northwest National Laboratory. The tellurium used in these experiments came from commercial sources. The gases used throughout the experiments were 99.995% purity NF_3 purchased from Air Liquide (Kennewick, WA) and 99.9995% argon purchased from Oxarc (Pasco, WA). Volatile tellurium hexafluoride (TeF_6) was produced in a modified Seiko thermogravimetric analyzer (TGA) model S200 with 5% NF_3 flow in argon at 50 mL/min total gas flow. Modifications that provide some protection from corrosive reactions on the interior of the TGA are described in earlier reports.^{12,13} The TGA was ramped to 500 °C at 10 °C/min and held isothermally through the completion of the reaction with results similar to those previously reported.¹³

Mass spectra were collected by directly coupling the gas outlet of the TGA to a molecular leak inlet valve of a quadrupole mass spectrometer (QMS) (1.2 MHz, 19 mm rods, 500 amu range; Extrel CMS, Pittsburgh, PA) with an EI source (tungsten filament). The mass spectrometer was arranged to sample gas directly from the outgas line of the TGA, through a heated line designed to prevent condensation of the tellurium species. The gas sampler for the mass spectrometer was arranged to introduce the sampled gas with minimum travel distance to the electron impact ionization source. Spectra were acquired in scanning profile mode at 250 amu/s and 19 microscans/acquisition. Reported spectra are the average of 101 consecutive acquisitions. A series of background spectra were taken before the TGA temperature ramp was started and were used to subtract the background from the TGA fluorination products' spectra.

Raman analysis of the TGA products was performed separately by cryogenically condensing (at -100 °C) the outgas products in a quartz optical cell as the gas exited the TGA. The cell was composed of two 1 cm path length UV cuvettes isolable from each other by Teflon stop cocks. Prior to experiments, argon gas was purged from the TGA through the gas cell, through an empty trap (to halt potential backflow), and then through a silicon oil bubbler to prevent air leakage. Condensed products were analyzed using an InPhotonics RS2000, high resolution Raman spectrometer with a thermoelectrically cooled charge-coupled detector (CCD) operating at -52 °C and a 670 nm, 150 mW diode laser as the excitation source. Laser power was focused through an InPhotonics Raman fiber optic probe operated in a 180° back reflection mode.

Density functional theory (DFT) electronic structure calculations were performed to elucidate the behavior of the ion fragments formed. All calculations were performed with the NWChem 6.5 computational chemistry program²⁵ with the B3LYP exchange-correlation functional^{26–29} and the Def2-TZVP basis and effective core potential for tellurium³⁰ and 6-311G++(3df, 3pd) basis for fluorine,³¹ respectively.

3. RESULTS AND DISCUSSION

Te metal and TeO_2 were used to produce TeF_6 by fluorination with 5% NF_3 in UHP argon in a TGA. Onset of TeF_6 production (observed by mass loss in the TGA and detection of product-related ions in the mass spectrometer) occurred

near 350 °C with production of the hexafluoride reaching 8 $\mu\text{mol}/\text{min}$ at 500 °C. The yield of TeF_6 produced was controlled by the amount of starting tellurium used in the experiment.

3.1. Raman Spectrum of TeF_6 . Raman spectroscopy was performed to verify the product of the reaction of Te metal and tellurium dioxide with NF_3 . When tellurium was reacted with NF_3 and the product was cryogenically condensed, a white solid was observed in the quartz optical cell along with a separate, unidentified red-violet solid. Upon removing the cryogenic bath and allowing the cells to return to room temperature, both solids were observed to sublime. The red-violet solid sublimed rapidly following removal of the cryogen. The white solid was observed to begin sublimation at approximately -35 °C. The behavior of the white solid was consistent with physical changes expected for TeF_6 .¹⁶ In addition, a separate white solid was observed to condense (without the need of cryogen) in the arm of the optical cell at the interchange between the TGA and quartz apparatus. This solid dissipated when exposed to air. Following exposure to air, the tube walls showed noticeable etching. This solid is consistent with earlier reports of dinitrosylhexafluorosilicate [$(\text{NO})_2\text{SiF}_6$] production.^{32,33} Despite earlier reports,^{34–38} spectrum acquisition under these conditions was found to be difficult, which is suspected to be due to transient heating of the sample from the Raman laser excitation source. Additional sources of difficulty were from the use of NF_3 rather than fluorine gas as the fluorinating agent, and possibly from the use of a continuous flow system rather than the typical condensation from a static system. The coproduction of the red-violet and white solids was consistent with early reports of pure NF_3 fluorinations of tellurium in quartz experimental apparatus at similar cryogenic temperatures.^{39–42}

To examine the nature of the red-violet solid, control experiments were also performed in which approximately 1000 Torr of NF_3 was heated in a stainless steel vessel without the presence of tellurium. When hot NF_3 exiting the 500 °C reactor was cooled directly into the Raman cell, a red-violet solid was collected, confirming that this product does not require tellurium to be produced, and is likely not part of the tellurium reaction being considered. After several heating and cooling cycles between -60 and -196 °C, which vaporized and condensed the material, the red-violet solid could not be recovered, and a viscous blue liquid condensed from the gas phase near -60 °C (Figure 1). Over time, as the sample was warmed to room temperature, a yellow-brown gas was observed in the cell (observed in both setups) which was confirmed by

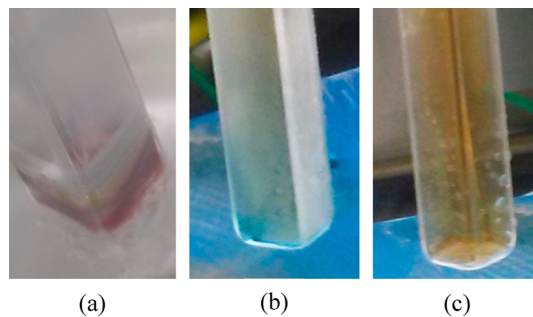


Figure 1. Nontellurium products cryogenically captured during NF_3 treatment: (a) unidentified red-violet solid; (b) unidentified blue liquid; (c) brown gas identified as NO_2 .

Raman spectroscopy as a mixture of NO_2 and N_2O_4 .⁴³ After further repetitions of the heating and cooling cycles, the blue liquid could no longer be recovered.

The production of NO_2 and N_2O_4 suggests a series of reactions from a reactive species that formed from hot NF_3 which is consistent with formation of nitrosyl fluoride (NOF) to produce nitrogenous oxides.^{32,44,45} Though unidentified, the behaviors of the red-violet solid and blue liquid suggest that these substances are related to this series of reactions. While the initiating species was either too short-lived or unstable to be a signature in the mass spectrum, the nitrogenous oxides all had to be considered as well as the fragmentation pattern of NF_3 itself in the assignment of background components. The mass spectrum of NF_3 and its EI fragmentation have been discussed.^{46,47}

Successful acquisition of the Raman spectrum of TeF_6 solid was accomplished by condensing the off-gas from the reaction of approximately 160 mg of Te metal with NF_3 , which produced sufficient material to avoid the previously described difficulties. Further, the Raman spectrum was acquired immediately to keep signal components of the side reactions to a minimum. Attempts were also made to obtain the Raman spectrum of the red-violet solid; however, the solid sublimed too readily for our apparatus to resolve its spectrum.

After the material was warmed to room temperature, only a white solid product could be obtained through use of cryogenic solutions at -100 and -196 °C. Raman spectra were collected and were consistent with spectra of tellurium hexafluoride reported in the literature^{34–38} with major peaks observed at 698, 669, and 319 cm^{-1} as shown in Figure 2. Minor peaks at

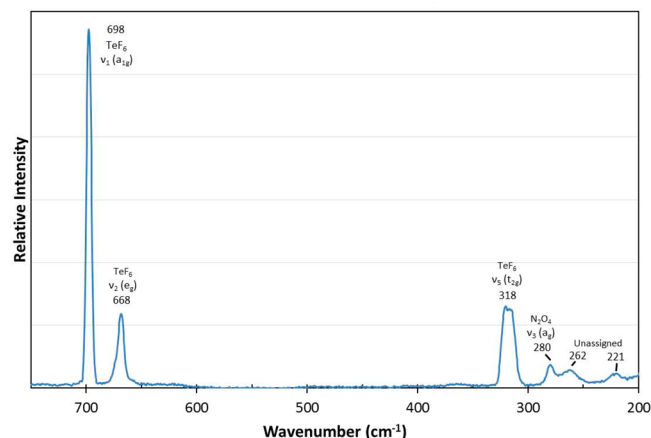


Figure 2. Observed Raman spectrum of solid TeF_6 captured from reacting NF_3 with Te metal.

280, 262, and 221 cm^{-1} are also observed. Following sublimation of the tellurium hexafluoride, additional peaks are observed which allowed identification of the 280 cm^{-1} peak as N_2O_4 .⁴³ The other peaks remain unidentified, but are likely due to contaminants from the additional NF_3 reaction with the quartz cell. At room temperature, no solid or liquid was observed in the cell. The boiling points of TeF_4 and $\text{F}_5\text{TeOTeF}_5$ are above room temperature which suggests that the only tellurium product present was the hexafluoride. The use of both Te metal and TeO_2 in these experiments indicates that di- or trimeric fluorides or oxyfluorides of tellurium as discussed in the literature²⁰ were not produced under our experimental conditions.

3.2. Mass Fragmentation of TeF_6 . Positive EI mass spectra resulting from the fluorination of Te metal or TeO_2 yielded similar results. Experiments showed that an electron energy of 35 eV gave the best total ion intensity. The spectrum resulting from the fluorination of Te metal is shown in Figure 3.

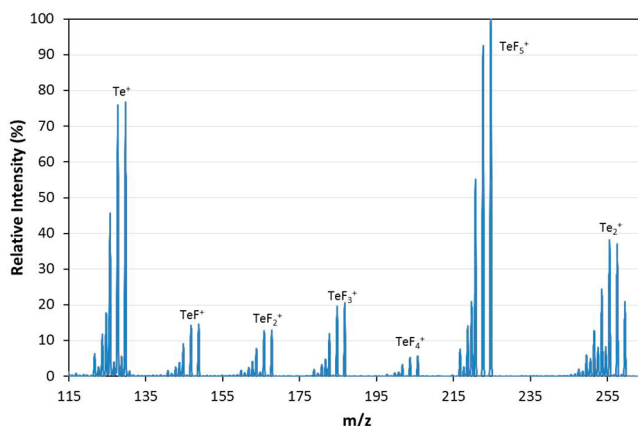


Figure 3. Positive EI mass spectrum of TeF_6 obtained through reaction of tellurium metal with NF_3 . Spectrum obtained with an electron energy of 35 eV.

The molecular TeF_6^+ ion was not observed. The ions Te^+ , Te_2^+ , TeF^+ , TeF_2^+ , TeF_3^+ , TeF_4^+ , and TeF_5^+ were all readily observed. All eight of the natural tellurium isotopes were accounted for in the Te^+ and TeF_5^+ series. The lowest abundance (0.09%) Te-120 containing ions were not detected in the TeF^+ , TeF_2^+ , TeF_3^+ , and TeF_4^+ series. Figure 4 shows the spectrum of the resulting TeF_5^+ series, and the resulting observed isotopic abundances are reported in Table 1.

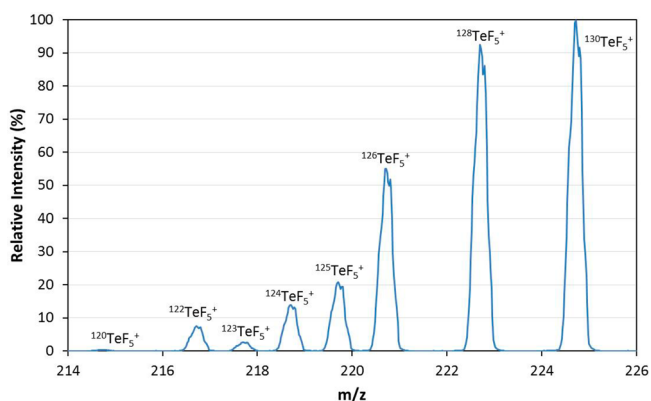
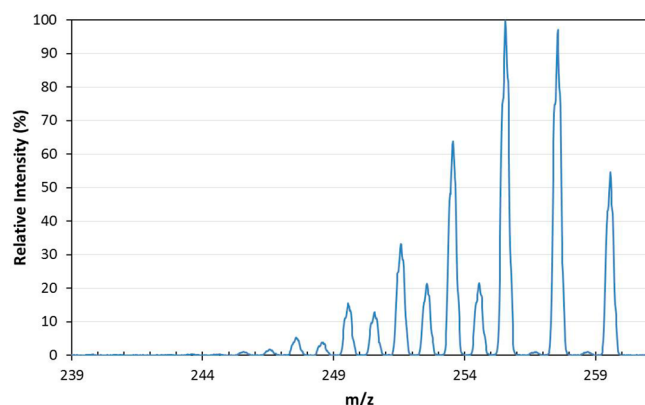


Figure 4. Positive EI mass spectrum of TeF_5^+ resulting from the ionization of TeF_6 obtained through fluorination of tellurium metal with NF_3 . Spectrum obtained with an electron energy of 35 eV.

3.3. Source of Te^+ and Te_2^+ . An additional signal from m/z 240 to 260 was also observed which was attributed to Te_2^+ formation. Figure 5 shows a relative intensity spectrum of this series, and calculated and measured abundances for each mass can be seen in Table 2. The literature reports the synthesis of only one tellurium dimer, Te_2F_{10} .^{17–19} Recent research suggests that this compound was never synthesized and was actually bis(pentafluorotelluryl) oxide ($\text{F}_5\text{TeOTeF}_5$).²⁰ If the ditellurium ions that were observed resulted from direct ionization and fragmentation of $\text{F}_5\text{TeOTeF}_5$, an oxygen atom would be

Table 1. Calculated and Observed Isotopic Abundance of Natural Te Based on TeF_5^+

isotope	abundance of natural Te (%)	relative abundance of natural Te (%)	measured relative abundance (%) ^a
130	34.1	100	100
128	31.8	93.1	92.5
126	18.8	55.3	55.1
125	7.1	20.7	20.9
124	4.7	13.9	14.0
123	0.9	2.6	2.6
122	2.6	7.5	7.6
120	0.1	0.3	0.3

^aCalculated using TeF_5^+ series from Te metal.**Figure 5.** Positive EI mass spectrum of Te_2^+ resulting from the ionization of TeF_6 obtained through fluorination of tellurium metal with NF_3 . Spectrum obtained with an electron energy of 35 eV.

bridging the tellurium atoms and fragments with oxygen incorporated would be observed elsewhere in the spectrum.

Consequently, these observations disfavor the argument for formation of an oxyfluoro dimer by direct fluorination methods under our experimental conditions.²⁰

Tellurium metal (melting point = 450 °C) has been shown to slowly volatilize and transfer down a tube within our temperature range.⁴⁸ As Te_2 is the more stable state for tellurium in the gas phase,^{49,50} both Te^+ and Te_2^+ ions would be observed in the mass spectrum if unfluorinated tellurium was reaching the mass spectrometer. When tellurium metal was heated in the absence of NF_3 , a mass loss was observed. However, no tellurium mass signal was observed. Additionally, when the ionization energy was lowered to 10 eV, TeF_x^+ ions were no longer observed, while Te^+ and Te_2^+ remained virtually unchanged. This final observation suggests that the ditellurium ions and the majority of the Te^+ ions are not the direct result of fragmentation from TeF_6 ionization. Two hypotheses for this set of signal observations are considered.

First, TeF_6 could react with the internal parts of the transfer system resulting in the decomposition to tellurium metal closer to the mass spectrometer leak valve. This product could then volatilize as Te_2 and ionize in the mass spectrometer. After tellurium was reacted in our experimentation and no further signal was observed by mass spectrometry, the leak valve to the mass spectrometer was closed, and the transfer line was flushed with argon for several hours. The transfer line was then isolated from further gas flow and coupled to a vessel containing tellurium hexafluoride. When the leak valve to the mass spectrometer was opened, Te^+ and Te_2^+ were immediately observed. When the hexafluoride reached the mass spectrometer, TeF_x^+ species were observed as well as a spike in the amount of Te^+ and Te_2^+ . This suggests that TeF_6 is reacting with the stainless steel transfer line and decomposing to tellurium metal. However, the vapor pressure of tellurium⁵¹ appears insufficient to completely account for the observed signal of these two ions.

Table 2. Calculated and Observed Abundance of Te_2^+ Masses from Pairing of Isotopes

mass	isotopic combination		calcd abundance (%)	relative calcd abundance (%)	measured relative abundance ^a (%)
260	130–130		11.6	50.7	53.4
258	130–128		21.6	94.4	98.6
256	130–126	128–128	22.9	100	100
255	130–125		4.8	21.0	21.5
254	130–124	128–126	15.2	66.3	64.6
253	130–123	128–125	5.1	22.2	22.6
252	130–122	128–124	8.3	36.2	34.4
	126–126				
251	128–123	126–125	3.2	14.1	14.0
250	130–120	128–122	4.0	17.3	15.9
	126–124	125–125			
249	126–123	125–124	1.0	4.4	4.8
248	128–120	126–122	1.4	6.0	6.0
	125–123	124–124			
247	125–122	124–123	0.4	1.9	~1.7 ^b
246	126–120	124–122	0.3	1.2	~1.2 ^b
	123–123				
245	125–120	123–122	5.8×10^{-02}	0.3	
244	124–120	122–122	7.4×10^{-02}	0.3	
243	123–120		1.6×10^{-03}	7.0×10^{-03}	
242	122–120		4.6×10^{-03}	2.0×10^{-02}	
240	120–120		8.1×10^{-05}	3.5×10^{-04}	

^aCalculated using Te_2^+ series from Te metal. ^bEstimated from spectra.

Second, a tungsten filament was used as the electron ionization source in these experiments. This filament reaches temperatures between 1600 and 2700 °C.⁵² At these temperatures, tellurium hexafluoride could thermally decompose⁵³ to the metal and then ionize as Te^+ and Te_2^+ . We observed that the Te^+ and Te_2^+ ions appear and dissipate at the same rate as the other TeF_x^+ ions in the mass spectrum. If the first pathway (decomposition in the transfer line) was the primary pathway, we'd expect different rates of in growth and the signal for these ions to linger. This suggests that thermal decomposition is the primary mechanism.

3.4. Relative Abundance of TeF_6 Ion Fragments. Upon further investigation of the signals presented in Figure 3, there is an alternating abundance of even (Te^+ , TeF_2^+ , TeF_4^+ , and TeF_6^+) and odd (TeF^+ , TeF_3^+ , and TeF_5^+) fluoride species. In the odd series, ion formation favors species containing higher numbers of fluorine atoms ($\text{TeF}_5^+ > \text{TeF}_3^+ > \text{TeF}^+$). Conversely, in the even series, the presence of fewer fluorine atoms is favored for higher ion formation ($\text{Te}^+ > \text{TeF}_2^+ > \text{TeF}_4^+ > \text{TeF}_6^+$, not observed). The relative intensities of the different observed species are shown in Table 3. Since the

Table 3. Relative Abundance of Observed Te Species Collected from Approximately 25 fg/s TeF_6

species	relative abundance ^a (%)
Te^+	76.8
TeF^+	14.5
TeF_2^+	13.0
TeF_3^+	20.6
TeF_4^+	5.7
TeF_5^+	100
TeF_6^+	not observed
Te_2^+	38.2 ^b

^aCalculated using ¹³⁰Te species. ^bRatio of mass 256 to ¹³⁰Te⁺.

Raman data suggests that TeF_6 is initially the major tellurium reaction product, we believe that the absence of the observed molecular ion (TeF_6^+) is due to instability of the molecular ion.

DFT calculations were performed to test the hypothesis of the stability of the ionic fragments. The results of the calculations are summarized in Table 4. In a comparison of the spin multiplicities of the odd species, the ground state of TeF^+ is a triplet (~1.3 eV lower than the singlet), while TeF_3^+ and TeF_5^+ are singlets. All species in the even series resulted in doublet radical ions. The Te–F bond lengths for the odd series

show a decreasing trend from TeF^+ to TeF_5^+ indicating a stronger bond and greater stability, while the even series (TeF_2^+ and TeF_4^+) shows the opposite trend. The largest even species, TeF_6^+ , has five bond lengths comparable to the TeF_5^+ bond lengths with the exception of one long bond of 2.38 Å, and the overall structure is a very strained octahedral. This suggests that TeF_6^+ will readily decompose to TeF_5^+ and contribute to the increased observed abundance of TeF_5^+ . The bond length/stability analyses also provide an explanation for the similar abundances of the TeF^+ , TeF_2^+ , and TeF_3^+ species, respectively. With regard to Te_2^+ , this ion is a doublet and analogous to the O_2^+/O_2 pair; the ion is more stable than Te_2 . All optimized structures and coordinates are provided in the Supporting Information.

4. CONCLUSIONS

Tellurium hexafluoride (TeF_6) was formed by reacting Te metal or TeO_2 with NF_3 at approximately 500 °C in a thermogravimetric analyzer (TGA). The gas outlet of the TGA was directly coupled to a quadrupole mass spectrometer (QMS) with an electron ionization source. Formation of TeF_6 was confirmed through separate analysis by cryogenic capture of the tellurium fluorination product and analysis through Raman spectroscopy.

When gaseous TeF_6 is ionized with a 35 eV electron ionization source, the reported mass spectrum was observed which includes Te^+ , TeF^+ , TeF_2^+ , TeF_3^+ , TeF_4^+ , and TeF_5^+ . The molecular ion was not observed. In addition, ditellurium ions (Te_2^+) were observed. We currently explain these ions along with the majority of the Te^+ signal as due to thermal decomposition of the TeF_6 with the ionization source. An alternating abundance of even (Te^+ , TeF_2^+ , TeF_4^+ , and TeF_6^+) and odd (TeF^+ , TeF_3^+ , and TeF_5^+) fluoride species was also observed. The odd fluorine ion species favored more fluorine ($\text{TeF}_5^+ > \text{TeF}_3^+ > \text{TeF}^+$) while the even ion species favored less fluorine ($\text{Te}^+ > \text{TeF}_2^+ > \text{TeF}_4^+ > \text{TeF}_6^+$, not observed). We also performed electronic structure calculations of the different species to support our observations. The observed even/odd stability pattern was explained by the Te–F bond lengths of each species.

■ ASSOCIATED CONTENT

Supporting Information

Structures and Cartesian coordinates (in Å) of the various species. The Supporting Information is available free of charge

Table 4. Calculated Energies (in Hartrees), Bond Lengths, Bond Angles, Coordinations, and Multiplicities of the Various TeF_x^+ Species

species	energy (Hartrees)	Te–F bond length (Å)	F–Te–F bond angle (deg)	coordination	multiplicity
TeF^+ (S)	−367.589 39	1.857		linear	singlet
TeF^+ (T)	−367.636 68	1.856		linear	triplet
TeF_2^+	−467.535 14	1.847	96.3	bent	doublet
TeF_3^+	−567.444 77	1.834	95.7	trigonal pyramid	singlet
TeF_4^+	−667.232 95	1.898, 1.824	98.6, 96.0, 161.7	distorted tetrahedron	doublet
TeF_5^+	−767.101 87	ax 1.827, eq 1.819	90, 120, 180	trigonal bipyramidal	singlet
TeF_6^+	−866.875 29	1.810, 1.827, 1.831, 1.827, 1.831, 2.380	88.5, 88.6, 96.1, 167.9, 152.2, 103.9, 88.6, 103.9, 88.5, 96.1, 83.9, 76.2, 76.0, 83.9, 180.0	very distorted octahedral	doublet

on the ACS Publications website at DOI: 10.1021/acs.inorgchem.5b00342.

AUTHOR INFORMATION

Corresponding Author

*E-mail: richard.clark@pnnl.gov.

Notes

The authors declare no competing financial interest.

ACKNOWLEDGMENTS

This research was funded by Pacific Northwest National Laboratory (PNNL) utilizing Laboratory Directed Research and Development (LDRD) funds. Pacific Northwest National Laboratory is operated by Battelle Memorial Institute for the United States Department of Energy under DOE contract number DE-AC05-76RL1830. This research was performed under the Nuclear Forensics Postdoctoral Fellowship Program, which is sponsored by the U.S. Department of Homeland Security, Domestic Nuclear Detection Office, and the U.S. Department of Defense, Defense Threat Reduction Agency. All the calculations were performed using EMSL, a national scientific user facility sponsored by the U.S. Department of Energy's Office of Biological and Environmental Research and located at PNNL.

REFERENCES

- (1) Bilous, O.; Doneddu, F. *Chem. Eng. Sci.* **1986**, *41*, 1403–1415.
- (2) Upson, P. C. Isotopic Enrichment of Uranium. In *The Nuclear Fuel Cycle: From Ore to Waste*; Wilson, P. D., Ed.; Oxford University Press Inc.: New York, 1996.
- (3) Choppin, G.; Liljenzin, J.-O.; Rydberg, J. *Radiochemistry and Nuclear Chemistry*; Butterworth-Heinemann: Woburn, MA, 2002.
- (4) Olander, D. R. *Prog. Nucl. Energy* **1981**, *8*, 1–33.
- (5) Suvorov, I. A.; Tchel'tsov, A. N. *Nucl. Instrum. Methods Phys. Res., Sect. A* **1993**, *334*, 33–36.
- (6) Uhlíř, J.; Mareček, M. *J. Fluorine Chem.* **2009**, *130*, 89–93.
- (7) Mitkin, V. N.; Shavinsky, B. M. *J. Fluorine Chem.* **2009**, *130*, 117–121.
- (8) Inabinett, D.; Knight, T.; Adams, T.; Gray, J. *Prog. Nucl. Energy* **2014**, *76*, 106–111.
- (9) Rashid, K.; Krouse, H. R. *Can. J. Chem.* **1984**, *63*, 3195–3199.
- (10) Johnson, T. M. *Chem. Geol.* **2004**, *204*, 201–214.
- (11) Koeman, E. C.; Simonettie, A.; Chen, W.; Burns, P. C. *Anal. Chem.* **2013**, *85*, 11913–11919.
- (12) McNamara, B.; Scheele, R.; Kozelisky, A.; Edwards, M. *J. Nucl. Mater.* **2009**, *394*, 166–173.
- (13) Scheele, R.; McNamara, B.; Casella, A. M.; Kozelisky, A. *J. Nucl. Mater.* **2012**, *424*, 224–236.
- (14) Scheele, R. D.; McNamara, B. K.; Casella, A. M.; Kozelisky, A. E.; Neiner, D. *J. Fluorine Chem.* **2013**, *146*, 86–97.
- (15) McNamara, B. K.; Buck, E. C.; Soderquist, C. Z.; Smith, F. N.; Mausolf, E. J.; Scheele, R. D. *J. Fluorine Chem.* **2014**, *162*, 1–8.
- (16) *CRC Handbook of Chemistry and Physics*, 84th ed.; CRC Press: Boca Raton, FL, 2003–2004; pp 4–88.
- (17) Campbell, R.; Robinson, P. L. *J. Chem. Soc.* **1956**, 3454–3458.
- (18) Yost, D. M.; Claussen, W. H. *J. Am. Chem. Soc.* **1933**, *55*, 885–891.
- (19) English, W. D.; Dale, J. W. *J. Chem. Soc.* **1953**, 2498–2499.
- (20) Watkins, P. M. *J. Chem. Educ.* **1974**, *51*, 520–521.
- (21) Leddicotte, G. W. *The Radiochemistry of Tellurium*; NAS-NS 3038; National Academy of Sciences: Washington, DC, 1961.
- (22) Fischer, J.; Steunenbergh, R. K. *Chemical and Radiochemical Studies of Tellurium in Fluoride Volatility Studies*; ANL-5593; Argonne National Laboratory: Lemont, IL, 1956.
- (23) Jarvis, G. K.; Mayhew, C. A. *Chem. Phys. Lett.* **2000**, *320*, 104–112.
- (24) Jarvis, G. K.; Kennedy, R. A.; Mayhew, C. A. *Int. J. Mass Spectrom.* **2001**, *205*, 253–270.
- (25) Valiev, M.; Bylaska, E. J.; Govind, N.; Kowalski, K.; Straatsma, T. P.; Van Dam, H. J. J.; Wang, D.; Nieplocha, J.; Apra, E.; Windus, T. L.; de Jong, W. A. *Comput. Phys. Commun.* **2010**, *181*, 1477–1489.
- (26) Becke, A. D. *J. Chem. Phys.* **1993**, *98*, 5648–5652.
- (27) Lee, C.; Yang, W.; Parr, R. G. *Phys. Rev. B* **1988**, *37*, 785–789.
- (28) Stephens, P. J.; Devlin, F. J.; Chabalowski, C. F.; Frisch, M. J. *J. Phys. Chem.* **1994**, *98*, 11623–11627.
- (29) Vosko, S. H.; Wilk, L.; Nusair, M. *Can. J. Phys.* **1980**, *58*, 1200–1211.
- (30) Peterson, K. A.; Figgen, D.; Goll, E.; Stoll, H.; Dolg, M. *J. Chem. Phys.* **2003**, *119*, 11113–11123.
- (31) Krishnan, R.; Binkley, J. S.; Seeger, R.; Pople, J. A. *J. Chem. Phys.* **1980**, *72*, 650–654.
- (32) Glemser, O.; Biermann, U. *Chem. Ber.* **1967**, *100*, 1184–1192.
- (33) Atkins, R. M.; Broer, M. M. *J. Mater. Res.* **1988**, *3*, 369–374.
- (34) Yost, D. M.; Steffens, C. C.; Gross, S. T. *J. Chem. Phys.* **1934**, *2*, 311–316.
- (35) Gaunt, J. *Trans. Faraday Soc.* **1953**, *49*, 1122–1131.
- (36) Claassen, H. H.; Goodman, G. L.; Holloway, J. H.; Selig, H. J. *J. Chem. Phys.* **1970**, *53*, 341–348.
- (37) Bosworth, Y. M.; Clark, R. J. H.; Rippon, D. M. *J. Mol. Spectrosc.* **1973**, *46*, 240–255.
- (38) Reynolds, D. J. The Vibrational Spectra of Inorganic Fluorides. In *Advances in Fluorine Chemistry*; Tatlow, J. C., Peacock, R. D., Hyman, H. H., Eds.; Butterworths: London, 1973; Vol. 7, pp 1–68.
- (39) Johnson, F. A.; Colburn, C. B. *J. Am. Chem. Soc.* **1961**, *83*, 3043–3047.
- (40) Streng, A. G.; Kirshenbaum, A. D.; Grosse, A. V. *Addition and Substitution Products of Oxygen Fluorides*; Contract 3085 (01); Temple University: Philadelphia, 1962.
- (41) Colburn, C. B.; Johnson, F. A. *Inorg. Chem.* **1962**, *1*, 715–717.
- (42) Streng, A. G. *J. Am. Chem. Soc.* **1963**, *85*, 1380–1385.
- (43) Bolduan, F.; Jodl, H. J.; Loewenschuss, A. *J. Chem. Phys.* **1984**, *80*, 1739–1743.
- (44) *Gmelin Handbook of Inorganic Chemistry: Fluorine*; Springer: New York, 1986; Vol. 4, p 409.
- (45) Glemser, O.; Wegener, J.; Mews, R. *Chem. Ber.* **1967**, *100*, 2474–2483.
- (46) Herron, J. T.; Dibeler, V. H. *J. Res. Natl. Bur. Stand., Sect. A* **1961**, *65A*, 405–409.
- (47) Haaland, P. D.; Jiao, C. Q.; Garscadden, A. *Chem. Phys. Lett.* **2001**, *340*, 479–483.
- (48) Sen, S.; Bhatta, U. M.; Kumar, V.; Muthe, K. P.; Bhattacharya, S.; Gupta, S. K.; Yakhmi, J. V. *Cryst. Growth Des.* **2008**, *8*, 238–242.
- (49) *CRC Handbook of Chemistry and Physics*, 84th ed.; CRC Press: Boca Raton, FL, 2003–2004; pp 5–25.
- (50) Davydov, A. V.; Rand, M. H.; Argent, B. B. *CALPHAD: Comput. Coupling Phase Diagrams Thermochem.* **1995**, *19*, 375–387.
- (51) Brooks, L. S. *J. Am. Chem. Soc.* **1952**, *74*, 227–229.
- (52) Extrel, CMS, L.P. *Axial Molecular Beam Ionizer User Manual*; Extrel: Pittsburgh, PA, 2004.
- (53) Galkin, N. P.; Tumanov, Y. N. *Russ. Chem. Rev.* **1971**, *40*, 154–164.